Loss of endothelial barrier integrity in mice with conditional ablation of podocalyxin (Podxl) in endothelial cells

Angélica Horrillo[a,b,1], Gracia Porras[a,b], Matilde S. Ayuso[a,b] and Consuelo González-Manchón[a,b]

[a] Department of Cellular and Molecular Medicine, Centre of Biological Research-CIB, CSIC, Madrid, Spain

[b] CIBER de Enfermedades Raras (CIBERER), Madrid, Spain

[1] Present address: Unit of Medicine and Experimental Surgery, Hospital Gregorio Marañón, Madrid, Spain

Corresponding author: Consuelo González-Manchón, Department of Cellular and Molecular Medicine, Centro de Investigaciones Biológicas-CIB, CSIC, Calle Ramiro de Maeztu 9, 28040-Madrid, Spain. Tel.: +34918373112-4441; Fax: +34915360432; e-mail: cgmanchon@cib.csic.es

Abbreviations: EC, endothelial cell; MLEC, mouse lung endothelial cell; Podxl, podocalyxin; CD34, cluster of differentiation 34; HEV, high endothelial venule; Tie2, tunica intima endothelial kinase 2; LPS, lipopolysaccharide; MRI, magnetic resonance imaging; PECAM-1, platelet/endothelial cell adhesion molecule 1; ICAM-2, intercellular adhesion molecule 2; TNF, tumor necrosis factor; VEGF, vascular endothelial growth factor; ERM, ezrin-radixin-moesin; CRP, C-reactive protein; SD, supplementary data.

Abstract

Podocalyxin (Podxl) has an essential role in the development and function of the kidney glomerular filtration barrier. It is also expressed by vascular endothelia but perinatal lethality of *podxl*$^{-/-}$ mice has precluded understanding of its function in adult vascular endothelial cells (ECs). In this work, we show that conditional knockout mice with deletion of Podxl restricted to the vascular endothelium grow normally but most die spontaneously around three months of age. Histological analysis showed a nonspecific inflammatory infiltrate within the vessel wall frequently associated with degenerative changes, and involving vessels of different caliber in one or more organs. Podxl-deficient lung EC cultures exhibit increased permeability to dextran and macrophage transmigration. After thrombin stimulation, ECs lacking Podxl showed delayed recovery of VE-cadherin cell contacts, persistence of F-actin stress fibers, and sustained phosphorylation of the ERM complex and activation of RhoA, suggesting a failure in endothelial barrier stabilization. The results suggest that Podxl has an essential role in the regulation of endothelial permeability by influencing the mechanisms involved in the restoration of endothelial barrier integrity after injury.

Key words: podocalyxin; endothelial cell; vascular permeability; inflammation

Introduction

Podocalyxin (Podxl) is an extensively O-glycosylated and sialylated type I transmembrane protein, closely related to CD34 and endoglycan. It was originally described in kidney podocytes (Kerjaschki et al., 1984) playing an essential role in the development and function of the kidney glomerular filtration barrier (Doyonnas et al., 2001). Podxl is also normally expressed on vascular endothelial cells (ECs) (Horvat et al., 1986), megakaryocytes and platelets (Kerosuo et al., 2004; Miettinen et al., 1999) and in some subsets of neurons (Vitureira et al., 2005). Aberrant expression of Podxl has been demonstrated in a number of cancers (Casey et al., 2006; Schopperle et al., 2003; Somasiri et al., 2004). Recent reports have provided useful data on the role of extrarenal Podxl. Platelet Podxl is involved in the control of haemostasis (Alonso-Martín et al., 2010; Pericacho et al., 2011). In brain, it seems to play multiple roles in neural development (Nowakowski et al., 2010; Vitureira et al., 2010). Podxl is not essential for hematopoiesis, but it may facilitate the crossing of endothelial barriers during migration to distant hematopoietic microenvironments (Doyonnas et al., 2005). Finally, overexpression of Podxl in cancer cells is associated with poor prognosis and metastasis (Boman et al., 2013; Dallas et al., 2012).

One of the most intriguing questions of Podxl research that remains unclear is whether the presence of this protein in ECs has pathophysiological relevance. Podxl is a widespread component of ECs in blood vessels of all calibers in a number of organs (lung, heart, small intestine, pancreas, kidney), but it is absent in the sinusoidal capillaries of liver and spleen (Horvat et al., 1986; Miettinen et al., 1990). In the specialized postcapillary high endothelial venules (HEV), Podxl was identified as one of the ligands for L-selectin (Sassetti et al., 1998). The apparently normal development of vascular ECs in Podxl-deficient mice was attributed to functional compensation by other sialomucins, such as CD34 (Doyonnas et al., 2001). Later, it was suggested that localization of Podxl at the endothelial cell-cell contacts is important to define the luminal cell surface during aorta development (Strilic et al., 2009). However, perinatal lethality of *podxl*$^{-/-}$ mice has precluded full understanding of its biological functions in adult vascular ECs.

We have recently generated a Podxl "floxed" mouse line in which *podxl* alleles carry loxP sites flanking a DNA fragment comprising exons 5-7 (Nowakowski et al., 2010; Pericacho et al., 2011). In the present work, to determine whether Podxl plays a role in regulating EC functions, these mice were crossed with the Tie2-Cre mouse line that produces Cre recombinase in endothelial and some hematopoietic cells (Kisanuki et al., 2001). We show evidence indicating that Podxl expression in ECs is essential for the maintenance of endothelial barrier integrity *in vivo* as well as *in vitro*. Podxl-deficient mice develop severe vasculitis leading to organ failure and premature death. In addition, permeability and macrophage transmigration were significantly increased in Podxl-deficient monolayers of lung ECs. The results suggest that Podxl is required to reestablish vascular integrity by ensuring proper cell-cell junctions.

Methods

Animals

Mice (Mus musculus) used in all the experiments were maintained under controlled conditions of light and temperature. Podxl$^{f/f}$::Tie2-Cre littermates were generated on a mixed CD1;129-P genetic background. To generate mice with a restricted deletion of *Podxl* in endothelial cells, mice homozygous for the floxed allele (with exons 5-7 flanked by functional loxP sites) generated previously (Nowakowski et al., 2010) were backcrossed for 10 generations with CD1 mice and crossed to Tie2-Cre mice (kindly gifted by Dr. J. L. de la Pompa, National Centre of Biotechnology, Madrid, Spain) (Kisanuki et al., 2001).

All experiments with animals were done in such a way as to minimize animal suffering, according to relevant national and international guidelines. Animals were killed by cervical dislocation under anesthesia by 3% isoflurane inhalation. The ethics committee of the Center for Biological Research

(CSIC) and the grant review board (ANEP) of the Spanish Ministry of Science and Technology specifically approved this study in accordance with the Directive 2010/63/EU of the European Parliament.

Some "floxed" (control mice) and Podxl-deficient mice (KO mice) were treated with intraperitoneal injection of phenol-purified lipopolysaccharides (LPS) from E. coli (Sigma), at a dose of 10-40 mg/Kg in a volumen of 100 μL PBS. Control animals were injected with the same volume of PBS.

PCR genotyping

For littermate genotyping, tail genomic DNA and oligonucleotides S-exon7: 5'-CTTGTTGCTGCCCTCTACGGCTGC-3' and AS-intron7: 5'-CCACATTTGAGTCTCCAGCGTTAG-3' were used to verify amplification of a 253 bp-DNA fragment comprising the right loxP sequence, and identification of Cre+ mice was performed by amplification of a DNA fragment with a sense oligonucleotide (5'-GGGAAGTCGCAAAGTTGTGAGTT-3') targeting a sequence of the Tie2 promoter and an antisense primer (5'-CTAGAGCCTGTTTTGCACGTCC-3') targeting the *Cre* gene sequence.

RT-PCR analysis of Podxl expression

Total RNA from mouse lung endothelial cells (MLECs) and platelets was obtained using the "High Pure RNA Isolation Kit" from Roche. RT-PCR amplification with oligonucleotides S-exon4: 5'-GTGAACCTCCCATAAGGCCAG-3' located in exon 4 and AS-exon8: 5'-TGTCCAGAGGGACGATCCAA-3' located in exon 8 confirmed normal sized cDNA in MLECs and platelets from "floxed" mice (control mice) and the deletion of exons 5-7 in cells from Cre+ mice (KO mice). Relative quantification of the normal Podxl mRNA transcript was assessed by real time RT-PCR using oligonucleotides S-exon7: 5'-CCTTCCTGCTCCTTGTTGCTG-3' and AS-exon8. In all RT-PCR assays, amplification of a cDNA fragment of mouse β-actin was carried out in parallel to verify that equal amounts of RNA were used ensuring correct normalization of Podxl expression.

Serum and urine biochemistry

Serum was obtained from non-citrated-blood samples. Blood was collected through cardiac puncture and stored overnight at 4ºC to permit complete blood coagulation. Serum was separated by centrifugation at 1500 g for 5 minutes. Serum and urine samples from 3-month old mice were biochemically analyzed to study cardiac and renal parameters (Hitachi 917, RCV Laboratories). Urine volume was determined using metabolic cages in two matched groups of six control and six Podxl-deficient mice with an equal number of males and females. Urinary protein and glucose excretion were measured in two 48-hour urine samples.

Tail-cuff measurement of blood pressure

Systolic and diastolic blood pressure was measured in 3-month old mice using the non-invasive computerized tail-cuff system BP-2000 (Visitech Systems, Cary, NC)**.** Conscious mice were trained for 4 days before starting the measurement to prevent stress. Arterial pressure as well as heart rate was measured during 10 consecutive days, with at least 20 determinations per day.

Magnetic resonance image

The lumen of the abdominal aorta was analyzed by magnetic resonance imaging (MRI) in three control and three KO mice of 3 months of age, using a 7 Tesla Bruker Pharmascan (Bruker Medical Gmbh, Ettlingen, Germany). Fourteen axial slices between the diaphragm muscle and the common iliac arteries were acquired and the area corresponding to the vascular lumen in each section was analyzed using the ImageJ software.

Thrombogenesis *in vivo*

As previously reported (Pericacho et al., 2011), 100 μL of blood was collected from one of the jugular veins of anesthetized mice into a tube containing 10 μL of 0.129 mol/L sodium citrate. A mixture of collagen/epinephrine (150 ng collagen type I (Chronolog) and 15 ng epinephrine (SIGMA) per g of mice body weight) was then injected into the same vein and, after 2 minutes, blood was withdrawn from the other jugular vein as indicated above. The number of platelets in both samples was determined using a hemocytometer analyzer Abacus Junior (Diatron Messtechnik GmbH, Austria).

Histological analysis

Tissue samples were collected immediately after euthanization and were fixed overnight in 4% paraformaldehyde, dehydrated, and paraffin-embedded. Serial 3-μm histological sections were prepared according to standard protocols and stained with hematoxylin/eosin for light microscopy. Histological analysis was performed blinded to the genotype by pathologists of Department of Pathology at the University of Santiago de Compostela. The following features were considered to define histopathological lesions: (1) Vasculitis/arteritis: the main histopathologic feature to define arteritis was the presence of an inflammatory infiltrate within the vessel wall. Disruption of the endothelial lining and the presence of edema together with inflamatory cells were also found. (2) Myocardial degeneration: disorganization of architecture of myocardial fibers, overgrowth of interstitial fibrous tissue, and necrosis areas. (3) Bronchopneumonia nonsuppurative: alveolar edema and accumulation of inflammatory cells in the alveolar wall and surrounding pulmonary vessels. (4) Mild glomerulonephritis: mild but significant increase of cellularity in renal glomeruli (proliferative

glomerulitis). (5) Hepatic micronecrosis: Unstructured small eosinophilic areas devoid of nuclei and surrounded by inflammatory cells.

Immunofluorescence detection of Podxl and PECAM-1 in kidney sections was carried out by sequential staining with goat polyclonal anti-Podxl (AF1556, R&D) and anti-PECAM-1 (sc-1506, Santa Cruz Biotechnology) antibodies.

Mouse lung endothelial cell isolation and culture

To prepare mouse lung endothelial cell (MLEC) cultures from 2-3 control or KO aged 3-months we introduced some modifications to previously described protocols (Fehrenbach et al., 2009). Briefly, animals were anesthetized with isofluorane, euthanized by dislocation, and dissected. First 5 mL of cold medium were injected into the right ventricle to flush the lung of blood cells and, then, 2 mL of 1.5 mg/mL collagenase A (Roche) was rapidly instilled through the trachea into the lungs. The lungs were removed and incubated with 6 ml of collagenase A in a 50-ml tube for 30 minutes in a 37°C water bath and gentle agitation every 10 minutes. After adding 25 ml of PBS, the tube was then shaken vigorously for 30 seconds and the resulting tissue/cell suspension was sieved through a 70-μm cell strainer and centrifuged for 5 minutes at 1000 rpm. The cell pellet was washed once with complete DMEM and, then, resuspended in 5 mL of the same medium and plated into a gelatin-coated 100 mm-plate. Resuspended cells from one or two more animals were seeded in the same plate. After 24 hours, the medium was changed to 50% DMEM-50% Hams F-12 medium supplemented with penicillin/streptomycin, 20% fetal bovine serum, 20 μg/mL endothelial cell growth supplement from bovine neural tissue (ECGS, Sigma) and 0.1 mg/mL heparin sodium salt (Sigma), and the cells cultured for 2 days. Cells were then removed by trypsin and purified by a single positive sorting using anti-ICAM-2 antibody (553326, BD Pharmigen) previously coupled to sheep anti-rat IgG Dynabeads (Invitrogen) and a magnetic particle concentrator (Dynamag^{TM}-15, Invitrogen 123.01D). Endothelial cells were plated on gelatin-coated 60 mm dishes and cultured during 3 days. After confluence, a second purification round was performed and cells plated into a 100 mm-plate. The endothelial identity and purity of the cells was confirmed by flow cytometry analysis (Coulter, model EPICS XL) of bound anti-ICAM-2 (557444) and anti-PECAM-1 (558738) from BD Pharmigen, and only cultures with percentages greater than 95% of endothelial cells were used for experiments.

***In vitro* vascular permeability assays**

$5x10^4$ MLECs were seeded and grown to confluence on collagen-coated transwell inserts (Millipore, ECM642). Cells were starved during 6 hours in medium containing 0.5% FBS and, then, treated with 100 ng/mL rmTNFα (Immunotools), 5 UI/mL thrombin (Sigma) or 250 ng/mL rmVEGF (Immunotools) for 4 hours. Finally, FITC-dextran (1:40) was added on top of the cells and, after 20

minutes at room temperature, fluorescence in the lower chamber was determined using a Varioskan plate reader (Thermo Scientific).

Human umbilical vein endothelial cells (HUVECs) cells were grown in EBM-2 medium supplementd with EGM-2 SingleQuots (Lonza). 10^6 cells at passage 3 were transfected using the Amaxa nucleofector system with 30 pmol of Podxl-specific or scrambled siRNAs (Ambion) and, them, 0.25 x 10^3 cells were seeded on colagen-coated transwell inserts and grown for a total period of 48 hours. Cells were treated with 100 ng/mL rhTNFα (R&D) for 16 hours, and with 250 ng/mL rhVEGF (Immunotools) or 100 ng/mL LPS (Sigma) for 2 hours. Then, FITC-dextran (1:20) was added and, after 1 hour, fluorescence was determined in the low chamber.

***In vitro* leukocyte transmigration assay**

The murine macrophage cell line PU5-1.8 was cultured on 75 cm^2 flasks with DMEM medium supplemented with 20% FBS and penicillin/streptomycin. 5x10^4 MLECs were grown to confluence on gelatine-coated 96-transwell plates (Corning, 3388) and starved during 4 hours in serum-free medium containing 0.1% BSA. The lower chamber was filled with medium plus 100 ng/mL TNFα, 5 UI/mL thrombin, or 250 ng/mL VEGF as chemoattractants and 10^5 macrophagic cells were added to the endothelial culture. Cells were incubated at 37ºC for 2 hours and, then, macrophages in the lower chambers of transwells were counted in a flow cytometer (Coulter flow cytometer model EPICS XL).

***In vivo* pulmonary vascular permeability**

A modification of the Miles assay was used to quantify vascular permeability in five control and five KO mice (Moitra et al., 2007). Briefly, mice were injected via the lateral tail vein with 25 mg/kg Evan's blue dye (EBD) 1 hour before sacrifice. After perfusion and sacrifice under isoflurane anesthesia on a mask, lung tissue was excised and EBD remaining in 100 mg of air-dried tissue parenchyma was extracted in formamide for 24 hours at 55ºC. The optical density of the supernatants was read at 620 nm on a spectrophotometer.

Immunofluorescence microscopy of endothelial cells

5x10^4 MLECs were grown to confluence on gelatin-coated glass-bottom plate dishes (MatTek Corporation). Cells were fixed with 4% paraformaldehyde, blocked and permeabilized with 0.5% Triton X-100 in PBS-0.5% BSA, and incubated overnight at 4ºC with goat polyclonal anti-Podxl (AF1556, R&D), rabbit polyclonal anti-VE-cadherin (PA5-19612, Thermo Scientific), rabbit monoclonal anti-β-catenin (ab32572, abcam), rabbit monoclonal anti-moesin (ab52490, abcam), or rabbit polyclonal anti-ERM-P (anti-phospho-ezrin(thr567)/radixin(thr564)/moesin(thr558) (AB3832, Millipore). After washing, cells were incubated with secondary antibodies conjugated with Alexa Fluor 488 or 546 for 1 hour at room temperature. When indicated, phalloidin-Alexa Fluor 568 was

added to the secondary antibody mixture to visualize the actin cytoskeleton. For nuclei labeling, cells were incubated with 1 μg/mL Hoechst or DAPI solution for 5 minutes at room temperature. Sequential incubation was performed when cells were labeled with primary antibodies raised in the same species. Cells were washed with PBS and visualized using the Leica TCS-SP5 confocal microscopy system.

Western and flow cytometry analysis

25 μg of protein lysate of MLECs from "floxed" control or Podxl-deficient mice were analyzed by western blot with goat polyclonal anti-Podxl (AF1556, R&D Systems), rabbit polyclonal anti-VE-cadherin (PA5-19612, Thermo Scientific), rabbit polyclonal anti-claudin-5 (sc-28670, Santa Cruz), rabbit polyclonal anti-ERM-P (AB3832, Millipore), and rabbit monoclonal anti-moesin (ab52490, abcam).

20 μg of protein lysate from HUVEC cells nucleofected with Podxl-specific or scrambled siRNAs were analyzed with anti-human Podxl (NBP2-25219, Novusbio) and anti-VE-cadherin (PA5-19612, Thermo Scientific).

Surface protein expression was assessed analyzing the binding of rat anti-ICAM-2 (557444) and anti-PECAM-1 (558738) from BD Pharmingen, and rat anti-CD34 (14-0341, eBioscience) to 25,000 MLECs.

Rac 1 and RhoA activation assays

MLECs were plated on 6 or 12-well plates coated with 5 μg/mL fibronectin. When cells reached 70-80% confluence, they were starved of serum for 16 hours prior stimulation with 1 U/mL thrombin for the indicated periods of time. Cells were rinsed and lysed, and equal amounts of protein (100-150 μg) were used for determination of GTPase activity of Rac1 and RhoA with the activation assay kits from Millipore (Temecula, CA) and Cytoskeleton (Denver, CO), respectively, and following manufacturer's instructions. Precipitated GTP-bound Rac1 and RhoA GTPases were separated by SDS-PAGE and detected by immunoblotting with specific mAbs. Total GTPases present in cell lysates was determined in a 20 μL of lysate sample, removed prior to pull-down. The relative amount of active GTPases was determined by densitometry using Image J free software (NIH).

Statistical analysis

Kaplan-Meier analysis and log rank test were performed to compare survival of mice groups, using the lifetest procedure of SAS version 9.4 (SAS Institute, Cary NC). For other measurements, data for the two groups of animals were analyzed using Student's t-test. The values are expressed as mean ± SD. Differences were considered statistically significant if $p \leq 0.05$.

Results

Deletion of Podxl in mouse endothelial cells (ECs)

To study the function of podocalyxin (Podxl) in ECs we bred mice harboring *podxl* alleles carrying exons 5-7 flanked by *lox*P sites (*podxl*$^{f/f}$) (Nowakowski et al., 2010) with mice expressing Cre recombinase under the control of the tunica intima endothelial kinase 2 (Tie2) promoter (Kisanuki et al., 2001) to generate *podxl*$^{f/f}$Tie-Cre mice.

We performed RT-PCR to evaluate the expression of Podxl in mouse lung ECs (MLECs) from "floxed" (control) and Cre+ (KO) mice. Since both Podxl and Tie2 are also expressed in the megakaryocytic lineage (Horvat et al., 1986; Saulle et al., 2012; Schlaeger et al., 2005), we also analyzed the expression of Podxl in platelets. As expected, in both cell types, amplification with oligonucleotides located in exons 4 and 8 rendered a product corresponding to the normal transcript in control mice and a product corresponding to the transcript with deletion of exons 5-7 in KO mice (Fig. 1A). Amplification using a sense-primer located in exon 7 rendered products corresponding to the normal transcript in both mouse lines (not shown), indicating incomplete effectiveness of Cre-mediated excision in the target lineages. By real-time RT-PCR we estimated that approximately 10% of MLECs expressed the Podxl normal transcript in KO mice (Fig. 1B).

Podxl expression at the protein level was assessed by immunofluorescence staining of histological sections of kidney and MLECs in culture. Confocal analysis revealed the presence of Podxl in glomeruli but not in the endothelium of blood vessels from KO mice (Fig. 1C). As described by other authors (Horvat et al., 1986; Strilic eta al., 2009), in mature vessel Podxl is distributed throughout the endothelial cell and, preferentially, localizes to the apical plasma membrane (Supplementary Data (SD) Fig. S1). Consistent with the levels of mRNA expression, the number of MLECs that express Podxl is markedly reduced in KO mice (Fig. 1C).

Phenotypic analysis of Podxl-deficient mice

Necropsy and histology.- Podxl-deficient mice are grossly indistinguishable from their littermate at birth. Both control and KO mice develop normally and have normal body weight. Although no obvious phenotypic abnormalities are observed in KO mice, most die spontaneously between 3 and 4 months of age (Fig. 2A). Necropsy analysis, performed in a period of 2-4 hours after death and without evident signs of autolysis, revealed widespread vascular and organ congestion (organs were swollen and showed hyperemic and edematous appearance) (Fig. 2B). Histological evaluation of individual tissues showed the presence of a non-specific arteritis/vasculitis involving vessels of different calibers in single or multiple organs (Fig. 3). Inflammatory infiltrates penetrate all layers of the arterial wall and can be quite variable in terms of severity and cell type. They were composed generally of mixed populations of mononuclear cells with few eosinophils, but predominance of polymorphs or a mixed population with abundance of eosinophils was also found in some locations.

Endothelial disruption and the presence of edema in the subendothelial space together with inflammatory cells were noted in some histological sections. In the heart, inflammatory infiltrates were associated with degeneration and necrosis of myocardial fibers and overgrowth of interstitial fibrous tissue. These degenerative features were often seen in the atrioventricular septum, at the base of papillary muscles, in the valves and, mainly, involving the root of blood vessels. Small necrotic foci (micronecrosis), characterized by eosinophilic areas devoid of the typical morphology and with few inflammatory cells, were frequently found in liver sections. The lung parenchyma shows inflammatory infiltrates in one or more layers of the vessel wall, perivascular lymphoid infiltrates, as well as edema and accumulation of inflammatory cells in the alveolar spaces (bronchopneumonia). Thickening of the interalveolar septa due to cellular infiltration was observed in some animals. Kidney sections revealed mild proliferative glomerulitis and, in some cases, the presence of amorphous, eosinophilic material in the urinary space. These lesions were also found in Podxl-deficient mice sacrificed at 3-4 months of age. The total number of mice analyzed was eleven (six males and five females) and the most common findings were arteritis/panarteritis (100%), myocarditis and myocardial degeneration (80%), bronchopneumonia nonsuppurative (80%), mild glomerulonephritis (60%), and hepatic micronecrosis (50%). No histological lesions were evident in any of the tissues examined in five newborn (Fig. 3) and five 1.5 month-old KO mice (not shown).

Biochemical analysis.- Plasma concentration of C-reactive protein (CRP) was significantly increased in KO mice (0.24+/-0.09 U/L and 45.21+/-18.91 U/L in control and KO mice, respectively). No significant differences between the two groups of mice were found in other biochemical markers of renal and cardiac dysfunction (SD Table S1). The volume of urine excreted in two matched groups of 6 control and 6 KO mice was not significantly different.

MRI analysis of aortic lumen area.- It has been reported that the diameter of the aortic lumen in Podxl-deficient embryos was less than half that of the control diameter (Strilic et al., 2009). In our study, the lumen of the abdominal aorta was analyzed by MRI in 3 control and 3 KO mice of 3-months of age. Fourteen axial slices between the diaphragm muscle and the common iliac arteries were acquired and the area corresponding to the vascular lumen in each section was analyzed using the ImageJ software. No significant differences were observed between control and KO mice in the average of the luminal area along the analyzed aortic region (SD Table S2).

Arterial pressure.- Given the possibility that the absence of Podxl produced endothelial dysfunction which impacts on vascular tone, we measured systolic (sBP) and diastolic (dBP) blood pressure in control (n=12, 6 males and 6 females) and KO (n=11, 5 males and 6 females) mice using the non-invasive tail-cuff procedure. sBP was found significantly elevated in two KO mice, one male and one female (141 and 144 mmHg, respectively, compared with 123$\pm$3.3 mmHg in the control mice).

Platelet function.- Consistent with the reduction in the expression of platelet Podxl and similarly to Podxl$^{f/f}$ PF4-Cre mice (Pericacho et al., 2011), Tie-Cre+ mice exhibited decreased systemic thrombosis in response to i.v. administration of platelet agonists (SD Fig. S2).

Lung function.- Pulmonary function testing was not performed, but symptoms of clear respiratory distress, consisting in arrhythmic and shallow rapid breathing, were observed in some mice shortly before dying. Necropsy analysis of these mice showed severe histological lesions in interalveolar septa and pulmonary vessels.

Increased sensitivity to LPS of Podxl-deficient mice

To evaluate the effects of Podxl deficiency on survival after LPS-induced endothelial barrier dysfunction, groups of mice received a single intraperitoneal injection of 10, 20, or 40 mg/Kg of LPS, and mortality was monitored over a 4-day period (Fig. 4). A markedly significant decrease of survival was observed in 9-10 week-old KO mice treated with 20 or 40 mg/Kg of LPS. Mortality of 5-6-week old KO mice was also higher than that of control group, but a significant difference was found only among those receiving 20 mg/Kg LPS. A cumulative endothelial lesion in older KO mice could explain this difference.

Deficiency of Podxl in ECs impairs their function *ex vivo*

The histological findings suggested a severe dysfunction of the vascular endothelial barrier in KO mice. To study the role of Podxl in controlling the integrity of the endothelial barrier we first developed an improved and reproducible method for isolation and culture of MLECs. This method yielded cell monolayers with more than 95% positive cells as assessed by flow cytometry measurement of ICAM-2 expression. Flow cytometry analysis revealed that Podxl-deficient MLECs from 3-month-old mice show surface expression levels of PECAM-1 and CD34 similar to control cells. However, a significant 10-20% increase in ICAM-2 surface labeling was observed in MLECs from KO mice (SD Fig. S3).

To investigate whether the absence of Podxl could alter *in vitro* endothelial monolayer permeability, we first used a FITC-dextran transwell assay. As shown in Fig. 5A, a significant increase of dextran movement was obtained in Podxl-deficient cells. This effect was observed in basal conditions as well as in cells stimulated with barrier-disruptive agonists such as VEGF, TNF-α, and thrombin. We next performed leukocyte transmigration assays and verified that the number of macrophagic PU5-1.8 cells that transmigrated through Podxl-deficient MLECs was significantly higher in both basal and stimulated experimental conditions (Fig. 5A). These data suggest that regulation of permeability and leukocyte transmigration through mouse microvascular ECs require Podxl. In accordance with these data, Evan's blue dye vascular leakage assays showed that lungs from KO mice exibited a significant increase in permeability (Fig. 5B).

To further confirm the effect of the absence of Podxl on permeability, Podxl expression was downregulated in HUVEC cells by transfection of Podxl-specific siRNAs. As shown in SD Fig. S4, Podxl-depleted HUVEC cells were more permeable to FITC-dextran in response to various barrier-disruptive stimuli.

Disassembly of adherens junctions in Podxl-deficient MLECs

Western analysis showed no differences in either VE-cadherin or claudin-5 in Podxl-deficient MLECs (SD Fig. S3). To investigate the consequence of Podxl deficiency in cadherin-mediated cell-to-cell contacts, we analyzed VE-cadherin staining in confluent monolayer cultures of MLECs treated with thrombin, which is known to induce a rapid and reversible disruption of endothelial intercellular junctions. Disruption of VE-cadherin staining was observed in both kinds of cells after thrombin stimulation; however, a continuous staining indicating restoration of the endothelial barrier was appreciated after 1-hour of treatment in control cells but not in Podxl-deficient cells (Fig. 5C). Besides inducing paracellular gaps, thrombin is known to rapidly stimulate F-actin fiber stress formation. As shown in Fig. 5D, F-actin stress fibers remained in Podxl-deficient cells but not in control cells 1-hour after thrombin stimulation.

The ERM (ezrin-moesin-radixin) family of actin-binding linkers participates in EC barrier modulation, being moesin is the most expressed ERM protein in a number of ECs (Adyshev et al., 2013). Total content of moesin were similar in control and Podxl-deficient cells (SD Fig. S3) but, as previously reported (Strilic et al., 2009), Podxl-deficient ECs showed a diffuse pattern of moesin distribution, in contrast to its accumulation at the cell-cell contacts in cells from control mice (Fig. 5E).

MLECs from both control and KO mice exhibited the highest levels of phosphorylated-ERM (ERM-P) immediately after detachment (SD Fig. S3). In fully spread cells, phosphorylation of ERM was transiently induced by thrombin. In contrast to control cells, ERM-P remained high after 45 minutes in Podxl-deficient cells (Fig. 6).

Podxl deletion alters the pattern of RhoA activation induced by thrombin

Junctional permeability is regulated by small GTPases (Spindler et al., 2010). LPS, thrombin, and VEGF increase activation of RhoA and endothelial permeability, and activation of Rac-1 and Cdc42 has been shown to stabilize the microvascular endothelial barrier. A significant difference was observed in the pattern of RhoA activation induced by thrombin between control and Podxl-depleted MLECs. As described in human ECs (Beckers et al., 2010), thrombin induced a rapid and transient activation of RhoA in MLECs. However, a longer sustained activation of RhoA was observed in Podxl-deficient cells (Fig. 6). In contrast to RhoA, no significant differential effects of thrombin were detected in Rac1 GTPase activation (Fig. 6).

Discussion

To study the functional significance of Podxl expression in endothelial cells (ECs), we bred mice bearing *lox*P-flanked alleles encoding Podxl (*podxl* $^{f/f}$) (Nowakowski et al., 2010) with mice expressing Cre recombinase under the control of the Tie2 promoter (Kisanuki et al., 2001) to generate *podxl*$^{f/f}$Tie2-Cre mice. Efficiency of Cre-mediated ablation of Podxl in lung ECs (MLECs), assessed by real time RT-PCR analysis of Podxl transcripts, showed 90% deletion of the *podxl* allele. Consistent with this, similar proportion of cells lacking Podxl was found by immunofluorescence analysis of MLECs in culture. Immunohistochemical staining of kidney sections revealed the presence of Podxl in glomeruli but not in the endothelium of blood vessels from Cre+ mice, indicating the specificity of the Cre-mediated ablation of *podxl* gene.

Podxl-deficient mice (KO mice) apparently grow normally but most die spontaneously at 3-4 months of age. According to histological analysis, they develop a nonspecific vasculitis that essentially consists in an inflammatory infiltrate within the vessel wall frequently associated with degenerative changes. These features were found in vessels of different caliber in all analyzed tissues, suggesting that efficient deletion of *podxl* in the vascular bed was generalized. The severity of myocardial and pulmonary infiltration could be the direct cause of death. The absence of pathologic findings in histological sections of euthanized newborn and 1.5-month old mice suggests that a gradually accumulated damage induced by the lack of Podxl precedes the onset of symptoms. Supporting this, compared with that of their age-paired controls, the sensitivity of 3-month old mice to LPS-induced endothelial barrier damage was higher than that of younger animals.

Since Podxl and Tie2 are both expressed in platelets, it cannot be ruled out that ablation of Podxl in platelets could eventually contribute to some of the pathological features. However, in our previously reported mouse model (*podxl*$^{fl/fl}$Pf4-Cre mice), in which Podxl deletion was restricted to platelets (Pericacho et al., 2011), no vascular-related lesions were found in deficient mice. Thus, the phenotype of *podxl*$^{fl/fl}$Tie2-Cre mice is basically due to the absence of Podxl in ECs. A marked increase in plasma levels of C-reactive protein (CRP) was detected in all analyzed KO mice. In humans, CRP is a known marker of inflammation and cardiovascular disease (Halim et al., 2014), and it is being also considered an active participant in the cardiovascular pathogenesis by promoting endothelial dysfunction (Bisoendial et al., 2010; Hein et al., 2009). In mice, CRP is not considered an acute-phase reactant but it can modulate the inflammatory response (Kapur et al., 2015). Therefore, it cannot be discarded the possibility that sustained high levels of CRP may exacerbate the disease in Podxl-deficient mice. No biochemical evidence of renal failure was detected in mice showing mild histological lessions in the kidneys. Other phenotypic abnormalities, such as increased blood pressure

and evident respiratory distress, were observed only in some animals. We can not rule out that hypertension detected in 2 of 11 KO animals was a casual finding. However, histological lesions found in mice with respiratory distress suggest that both findings are related and are due to the absence of Podxl. Podxl has been shown to be required for early vascular lumen formation (Strilic et al., 2009), but we could not detect a significant reduction in the lumen of abdominal aorta in KO mice.

In the total knockout model (Doyonnas et al., 2001), approximately 25% of the *podxl-/-* embryos obtained by Caesareas section exhibited mild to severe edema. Recently, in a mouse model with conditional ablation of *podxl* driven by the VE-cadherin promoter (Debruin et al., 2014), Podxl was shown to regulate murine lung vascular permeability by altering EC adhesion. In the present study, the severe histologic lesions of mice with more extensive deletion of Podxl in the vascular bed, besides reinforcing this notion, reveal an essential role of Podxl in the regulation of the endothelial barrier. Levels of CD34 were similar in control and Podxl-deficient ECs; thus, the loss of Podxl expression by the vasculature does not result in a compensatory increase in the expression of other related sialomucins, as previously suggested (Doyonnas et al., 2001).

To further explore the mechanism by which the lack of Podxl leads to vascular damage, we first developed an optimized procedure for obtaining of highly enriched EC cultures from pulmonary microvasculature of 3-month-old mice. Although expression of endothelial surface markers is conserved, Podxl-deficient cell monolayers exhibited a significant increase in basal permeability to dextran and inflammatory cells. Permeability was also higher in cells stimulated with endothelial barrier-disruptive agents such as thrombin. Migration through the junctions between adjacent ECs is the major pathway for leukocyte extravasation in several tissues (Shulted et al., 2011). Stability of cell contacts is mainly maintained by VE-cadherin, the main component of endothelial adherens junctions *in vivo* as well as *in vitro* (Shulted et al., 2011). Consistent with this, the immunofluorescence analysis of cell-cell contacts showed that after 1-hour treatment with thrombin, F-actin stress fibers and gaps in the VE-cadherin labelling remained only in Podxl-deficient cells, indicating that recovery of the barrier disruption induced by thrombin is delayed in the absence of Podxl. In agreement with these results, increased pulmonary vascular permeability was detected *in vivo* in KO mice.

Podxl is known to interact with the ezrin-moesin-radixin (ERM) complex, a family of actin-binding linkers that participate in EC barrier modulation (Adyshev et al., 2013). The abnormal distribution of moesin observed in Podxl-deficient MLECs was also reported in embryos of the Podxl total knockout mouse model associated to defective lumen formation during aorta development (Strilic et al., 2009). However, in the present study, *in vivo* determination of aortic cross-sectional area by MRI analysis did not reveal apparent difference between control and KO mice. It is possible that residual expression of Podxl due to incomplete Cre excision was sufficient to support normal lumen formation.

Consistent with the delayed restoration of VE-cadherin labeling and actin-based cytoskeleton, the

recovery of basal levels of phosphorylated ERM after thrombin stimulation was significantly slower in Podxl-deficient cells. The ERM proteins have been shown to act both upstream and downstream of the small Rho GTPases (Fehon et al., 2010). In human pulmonary artery endothelial cells (HPAEC), ERM proteins are critically involved in the thrombin-induced disruption of the endothelial barrier, and it has been shown that ERM phosphorylation can induce actin cytoskeleton changes and endothelial hiper-permeability via RhoA activation (Adyshev et al., 2013). In agreement with this, our study shows that persistent phosphorylation of ERM and delayed recovery of endothelial integrity in Podxl-deficient MLECs after thrombin stimulation was accompanied by sustained activation of RhoA. Although we do not provide a molecular mechanism for the role of Podxl in vascular permeability, the results clearly suggest that the lack of Podxl alters the intracellular signaling machinery responsible for restoring the endothelial barrier integrity after injury. Moesin is the most abundant component of the ERM complex in endothelial cells (Adyshev et al., 2013). It is possible that the altered distribution of moesin in KO cells ameliorates their recruitment and activation at the plasma membrane. This interpretation of the results would explain that appearance of pathological symptoms requires either prolonged exposure of the Podxl-deficient endothelium or a severe inflammatory stress like LPS administration.

In addition, mechanisms related with the adhesive and sialylation-dependent functions of Podxl could also be involved in the failure of the Podxl-deficient vascular endothelium. The role of Podxl in cell adhesion is controversial as both pro- and anti-adhesive functions have been described depending on cell type and glycosylation feature (Larrucea et al., 2007; Larrucea et al., 2008; Takeda et al., 2000), leading also to suggest that the amount of Podxl may regulate adhesion by altering the distribution and effects of other adhesion molecules on the cell surface (Nielsen and McNagny, 2009). Thus, it cannot be ruled out that the lack of Podxl resulted in exposure of normally hidden adhesion molecules, thereby increasing the quantity of leukocytes entering organs in both basal immune surveillance and inflammation. In agreement, increased exposure of surface ICAM-2 was consistently observed in Podxl-deficient MLEC cultures.

To our knowledge, this *podxl*$^{f/f}$Tie2-Cre mouse is the first genetically modified model resembling features of human vasculitis, a heterogeneous group of rare diseases with a common characteristic: inflammation of blood vessels walls. The pathogenesis of the disease is poorly understood and, in most of cases, treatment is symptomatic and directed to limit organ damage (Sharma et al., 2011). These mice might serve as a valuable tool for the study of vasculitis and the identification of molecules or mechanisms that may be relevant targets for controling vascular permeability changes associated with a number of diseases. Also, since mutations of *podxl* have been associated with human diseases (Barua et al., 2014; Casey et al., 2006), we raise the possibility that certain mutations may disrupt its endothelial barrier protective function and, consequently, be associated with some cardiovascular events.

In summary, the generation of mice with conditional ablation of the *podxl* gene restricted to vascular endothelium has revealed an essential role of Podxl in the control of vascular permeability. This control seems to be exerted by regulating the mechanism(s) involved in the restoration of barrier integrity after injury. Besides its utility for studying the function of Podxl in the vascular endothelium, this mouse model is a useful tool for the study of vascular inflammatory processes and identification of new drug targets.

Acknowledgments

We thank Tomás Fontela (Centro de Investigaciones Biológicas-CIB, CSIC) for his help with generation of *podxl*$^{f/f}$Tie-Cre mice.

This work was supported by grants SAF2007-61701 and BFU2010-15237 from the Secretaría de Estado de Investigación, Desarrollo e Innovación, and grant PIE 201020E018 from CSIC. Angélica Horrillo and Gracia Porras were supported by contracts from CIBER de Enfermedades Raras (CIBERER), an initiative of the Spanish Health Institute Carlos III (ISCIII).

Conflict of interest statement

The authors declare no conflict of interest.

References

Adyshev, D.M., Dudek, S.M., Moldobaeva, N., Kim, K.M., Ma, S.F., Kasa, A., García, J.G., Verin, A.D., 2013. Ezrin/radixin/moesin proteins differentially regulate endothelial hyperpermeability after thrombin. Am. J. Physiol. Lung Cell Mol. Physiol. 305, L240-255.

Alonso-Martín, S., Nowakowski, A., Larrucea, S., Fernández, D., Vilar-Egea, M., Ayuso, M.S., Parrilla, R., 2010. Overexpression of podocalyxin in megakaryocytes and platelets decreases the bleeding time and enhances the agonist-induced aggreagation of platelets. Thromb. Res. 125, e300-305.

Barua, M., Shieh, E., Schlondorff, J., Genovese, G., Kaplan, B.S., Pollak, M.R., 2014. Exome sequencing and in vitro studies indentified podocalyxin as a candidate gene for focal and segmental glomerulosclerosis. Kidney Int. 85, 124-133.

Beckers, C.M., van Hinsbergh, V.W., van Nieuw Amerongen G.P., 2010. Driving Rho GTPase activity in endothelial cells regulate barrier integrity. Thromb. Haemost. 103, 40-55.

Bisoendial, R.J., Boekholdt, S.M, Vergeer, M., Stroes, E.S.G., Kastelein, J.J.P., 2010. C-reactive protein is a mediator of cardiovascular disease. Eur. Heart J. 31, 2087-2095.

Boman, K., Larsson, A.H., Segersten, U., Kuteeva, E., Johannesson, H., Nodin, B., Eberhard, J., Uhlén, M., Malmström, P.U., Jirström, K., 2013. Membranous expression of podocalyxin-like protein is an independent factor of poor prognosis in urothelial bladder cancer. Br. J. Cancer. 108, 2321-2328.

Casey, G., Neville, P.J., Liu, X., Plummer, S.J., Cicek, M.S., Krumroy, L.M., Curran, A.P., McGreevy, M.R., Catalona, W.J., Klein, E.A., Witte, J.S., 2006. Podocalyxin variants and risk of prostate cancer and tumor aggressiveness. Hum. Mol. Gen. 15, 735-741.

Dallas, M.R., Chenm, S.H., Streppel, M.M., Sharma, S., Maitra, A., Konstantopoulos, K., 2012. Sialofucosylated podocalyxin is a functional E- and L-selectin ligand expressed by metastatic pancreatic cancer cells. Am. J. Physiol. Cell. Physiol. 303, C616-624.

Debruin, E.J., Hughes, M.R., Sina, C., Liu, A., Jian, Z., López, M., Lo, B., Abraham, T., McNagny, K.M., 2014. Podocalyxin regulates murine lung vascular permeability by altering endothelial cell adhesion. Plos One. 9, e108881.

Doyonnas, R., Kershaw, D.B., Duhme, C., Merkens, H., Chelliah, S., Graf, T., McNagny, K.M., 2001. Anuria, omphalocele, and perinatal lethality in mice lacking the CD34-related protein podocalyxin. J. Exp. Med. 194, 13-27.

Doyonnas, R., Nielsen, J.S., Chelliah S., Drew, E., Hara, T., Miyajima, A., McNagny, K.M., 2005. Podocalyxin is a CD34-related marker of murine hematopoietic stem cells and embryonic erythroid cells. Blood. 105, 4170-4178.

Fehon, R.G., McClatchey, A., Bretscher, A., 2010. Organizing the cell cortex: the role of ERM proteins. Nat. Rev. Mol. Cell. Biol. 11, 276-287.

Fehrenbach, M., Cao, G., Williams, J.T., Finklestein, J.M., DeLisser, H.M., 2009. Isolation of murine lung endothelial cells. Am. J. Physiol. Lung Cell. Mol. Physiol. 296, L1096-1103.

Halim, S.A., Newby, L.K., Ohman, E.M., 2014. Biomarkers in cardiovascular clinical trials: past, present, future. Clin. Chem. 58, 45-53.

Hein, V.H., Singh, U., Vasquez-Vivar, J., Devaraj, S., Kuo, L., Jialal, I., 2009. Human C-reactive protein induces endothelial dysfunction and uncoupling of eNOS in-vivo. Atherosclerosis. 206, 61-68.

Horvat, R., Hovorka, A., Dekan, G., Poczewski, H., Kerjaschki, D., 1986. Endothelial cell membranes contain podocalyxin, the major sialoprotein of visceral glomerular epithelial cells. J. Cell Biol. 102, 484-491.

Kapur, R., Kim, M., Shanmugabhavananthan, S., Liu, J., Li, Y., Semple, J.W., 2015. C-reactive protein (CRP) enhances murine antibody-mediated transfusion-related acute lung injury (TRALI). Blood. 2015;pii:blood-2015-09-672592.

Kerjaschki, D., Sharkey, D.J., Farquhar, M.G., 1984. Identification and characterization of podocalyxin-the major sialoprotein of the renal glomerular epithelial cell. J. Cell Biol. 98, 1591-1596.

Kerosuo, L., Juvonen, E., Alitalo, R., Gylling, M., Kerjaschki, D., Miettinen, A., 2004. Podocalyxin in human haematopoietic cells. Br. J. Haematol. 124, 809-818.

Kisanuki, Y.Y., Hammer, R.E., Miyazaki, J., Williams, S.C., Richardson, J.A., Yanagisawa, M., 2001. Tie2-Cre transgenic mice: a new model for endothelial cell-lineage analysis in vivo. Dev. Biol. 230, 230-242.

Larrucea, S., Butta, N., Rodríguez, R.B., Alonso-Martín, S, Arias-Salgado, E.G., Ayuso, M.S., Parrilla, R., 2007. Podocalyxin enhances the adherence of cells to platelets. Cell. Mol. Life Sci. 64, 2965-2974.

Larrucea, S., Butta, N., Arias-Salgado, E.G., Alonso-Martín, S., Ayuso, M.S., Parrilla, R., 2008. Expression of podocalyxin enhances the adherence, migration, and intercellular communication of cells. Exp. Cell Res. 314, 2004-2015.

Miettinen, A., Dekan, G., Farquhar, M.G., 1990. Monoclonal antibodies against membrane proteins of the rat glomerulus. Immunochemical specificity and immunofluorescence distribution of the antigens. Am. J. Pathol. 137, 929-944.

Miettinen, A., Solin, M.L., Reivinen, J., Juvonen, E., Vaisanen, R., Holthofer, H., 1999. Podocalyxin in rat platelets and megakaryocytes. Am. J. Pathol. 154, 813-22.

Moitra, J., Sammani, S., Garcia, J.G.N., 2007. Re-evaluation of Evans Blue dye as a marker of albumin clearance in murine models of acute lung injury. Transl. Res. 150, 253-265.

Nielsen, J.S., McNagny, K.M., 2009. The role of podocalyxin in health and disease. J. Am. Soc. Nephrol. 20, 1669-1676.

Nowakowski, A., Alonso-Martín, S., González-Manchón, C., Larrucea, S., Fernández, D., Vilar, M., Cerdán, S., Ayuso, M.S., Parrilla, R., 2010. Ventricular enlargement associated with the panneural ablation of the podocalyxin gene. Mol. Cell. Neurosci. 43, 90-97.

Pericacho, M., Alonso-Martín, S., Larrucea, S., González-Manchón, C., Fernández, D., Sánchez, I., Ayuso, M.S., Parrilla, R., 2011. Diminished thrombogenic responses by deletion of the podocalyxin gene in mouse megakaryocytes. Plos One. 6, e26025.

Sassetti, C., Tangemann, K., Singer, M.S., Kershaw, D.B., Rosen, S.D., 1998. Identification of podocalyxin-like protein as a high endothelial venule ligand for L-selectin: Paralles to CD34. J. Exp. Med. 187, 1965-1975.

Saulle, E., Guerriero, R., Petronelli, A., Coppotelli, E., Gabbianelli, M., Morsilli, O., Spinello, I.,

Pelosi, E., Castelli, G., Testa, U., Coppola, S., 2012. Autocrine Role of Angiopoietins during Megakaryocytic Differentiation. Plos One. 7, e39796.

Schlaeger, T.M., Mikkola, H.K., Gekas, C., Helgadottir, H.B., Orkin, S.H., 2005. Tie2Cre-mediated gene ablation defines the stem-cell leukemia gene (SCL/tal1)-dependent window during hematopoietic stem-cell development. Blood. 105, 3871-3874.

Schopperle, W.M., Kershaw, D.B., DeWolf, W.C., 2003. Human embryonal carcinoma tumor antigen, Gp200/GCTM-2 is podocalyxin. Biochem. Biophys. Res. Commun. 399, 285-290.

Sharma, P., Sharma, S., Baltaro, R., Hurley, J., 2011. Systemic vasculitis. Am. Fam. Physician. 83, 556-565.

Shulted, D., Küppers, V., Dartsch, N., Broermann, A., Li, H., Zarbock, A., Kamenyeva, O., Kiefer, F., Khandoga, A., Massberg, S., Vestweber, D., 2011. Stabilizing the VE-cadherin-catenin complex blocks leukocyte extravasation and vascular permeability. EMBO J. 30, 4157-4170.

Somasiri, A., Nielsen, J.S., Makretsov, N., McCoy, M.L., Prentice, L., Gilks, C.B., Chia, S.K., Gelmon, K.A., Kershaw, D.B., Huntsman, D.G., McNagny, K.M., Roskelley, C.D., 2004. Overexpression of anti-adhesin podocalyxin is an independent predictor of breast cancer progression. Cancer Res. 64, 5068-5073.

Spindler, V., Schlegel, N., Waschke, J., 2010. Role of GTPases in the control of microvascular permeability. Cardiovasc. Res. 87, 243-253.

Strilic, B., Kucera, T., Eglinger, J., Hughes, M.R., McNagny, K.M., Tsukita, S., Dejana, E., Ferrara, N., Lammert, E., 2009. The molecular basis of vascular lumen formation in the developing mouse aorta. Dev. Cell. 17, 505-515.

Takeda, T., Go, W.Y., Orlando, R.A., Farquhar, M.G., 2000. Expression of podocalyxin inhibits cell-cell adhesion and modifies junctional properties in Madin-Darby canine kidney cells. Mol. Biol. Cell. 11, 3219-3232.

Vitureira, N., McNagny, K., Soriano, E., Burgaya, F., 2005. Pattern of expression of the podocalyxin gene in the mouse brain during development. Gene Expr. Patterns. 5, 349-354.

Vitureira, N., Andrés, R., Pérez-Martínez, E., Martínez, A., Bribián, A., Blasi, J., Chelliah, S., López-Doménech, G., De Castro, F., Burgaya, F., McNagny, K., Soriano, E., 2010. Podocalyxin is a novel polysialylated neural adhesion protein with multiple roles in neural development and synapse formation. Plos One. 5, e12003.

Figures and legends

Figure 1

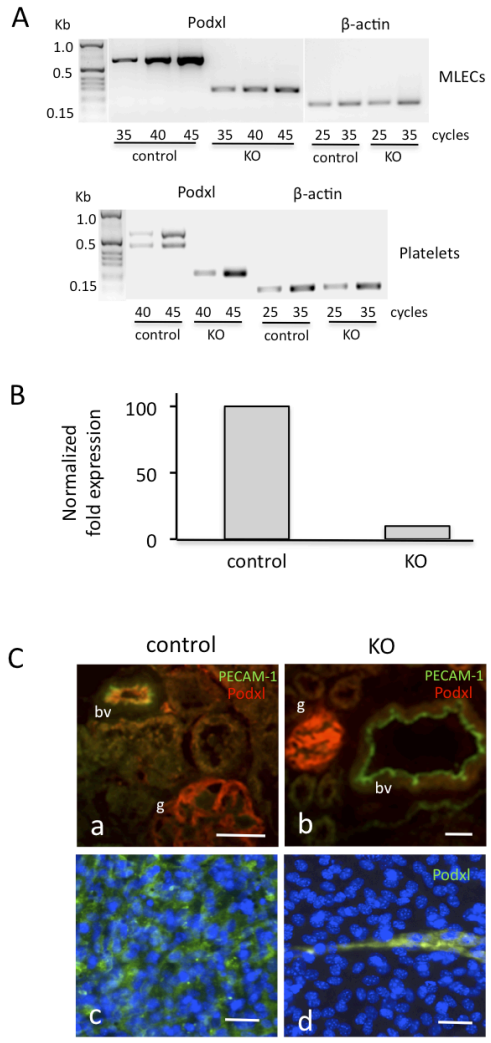

Figure 1. Podxl expression in "floxed" (control) and Cre+ (KO) mice. Total RNA was extracted from mouse lung ECs (MLECs) and platelets from three control and three KO mice, and the RNA mixture was used for RT-PCR amplification of Podxl and β-actin transcripts, as described in Methods. (A) Amplification with oligonucleotides located in exons 4 and 8 results in products of normal size in control mice and products with deletion of exons 5-7 in KO mice. (B) Relative expression of Podxl normal transcript in MLECs from control and KO mice was determined by real-time PCR using oligonucleotides located in exon 7 and 8. The results were quantified and normalized to β-actin expression and are the average of two independent experiments performed in triplicate with different RNA mixtures of three mice of each type. (C) Immunofluorescence detection of Podxl in kidney sections (a, b) and cultured MLECs (c, d) from control and KO mice. Nuclei were stained with DAPI

(blue). The assay was performed three times with similar results. In panel C, scale bars: 50 μm (a and b), 20 μm (c and d).

Figure 2

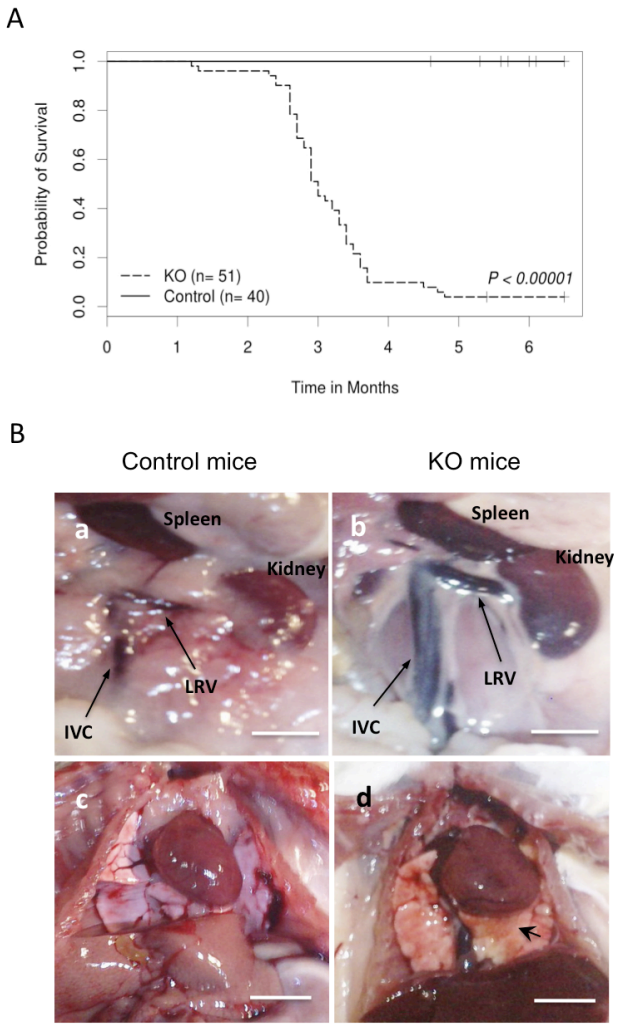

Figure 2. Survival and pathological findings in Podxl-deficient mice. (A) Kaplan-Meier survival curves of control and KO sibling mice of at least 10 litters from 5 different breeding pairs. In a sample of 51 KO mice, 25 mice (49%) died before 3 months, 21 (41%) between 3 and 4 months, 3 (6%) after 4 months, and only 2 mice (4%) were alive at 6 months of age. None of the 40 control mice died spontaneously within the first 6 months of life. As shown in the figure, 6 of these animals were euthanized after 4.5 months. (B) (a-b) Marked congestion of the inferior vena cava (IVC) and the left renal vein (LRV) in a KO mouse. (c-d) Pulmonary congestion in a KO mouse. Representative images obtained in necropsy analysis of more than ten mice. Scale bars: 0.5 cm.

Figure 3

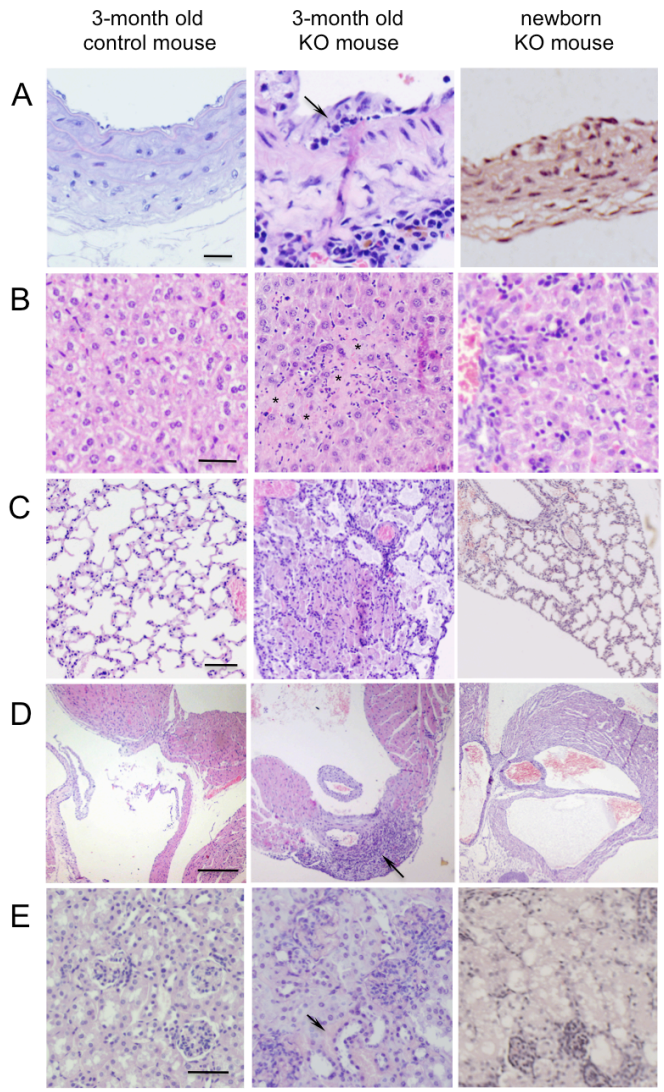

Figure 3. Histological lesions in Podxl-deficient mice. Representative images of hematoxylin and eosin (H&E)-stained tissue sections from control and KO mice. Alterations described below were found in tissues of eleven 3-month old KO mice but not in five KO newborns and five 3-month old control mice. (A) Subendothelial edema (arrow) and inflammatory cells infiltrating both the medial and adventitial layers in a pulmonary arteriole. (B) Inflammatory infiltrate surrounding necrotic areas (asterisks) devoid of nuclei in liver sections. (C) Alveolar edema and abundance of inflammatory cells in alveoli and surrounding pulmonary vessels, characteristics of non suppurative bronchopneumonia. (D) Heart section showing a severe myocardial infiltration of inflammatory cells (arrow) asymmetrically distributed around a large vessel (arrow). (E) Vascular congestion (arrow) and

significant increase of cellularity in renal glomeruli. Images were taken at 40x (A, B and E), 20x (C) or 10x magnification (D). Scale bars: 50 μm (A and B), 100 μm (C and E), and 400 μm (D).

Figure 4

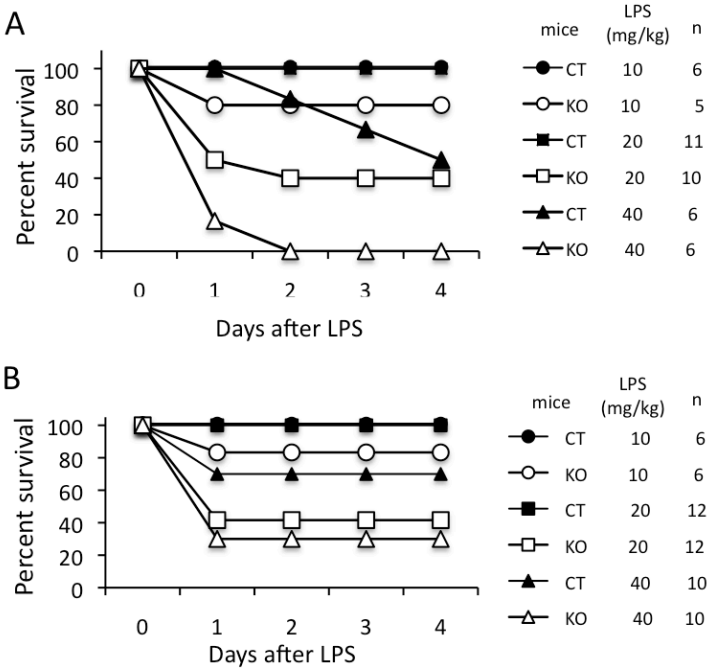

C

Group comparison	p values
CT vs KO mice (9-10 weeks, 10 mg/Kg LPS)	0.2733
CT vs KO mice (9-10 weeks, 20 mg/Kg LPS)	**0.0027**
CT vs KO mice (9-10 weeks, 40 mg/Kg LPS)	**0.0013**
CT vs KO mice (5-6 weeks, 10 mg/Kg LPS)	0.3170
CT vs KO mice (5-6 weeks, 20 mg/Kg LPS)	**0.0139**
CT vs KO mice (5-6 weeks, 40 mg/Kg LPS)	0.0810
10 vs 40 mg/Kg LPS (CT, 9-10 weeks)	0.0554
10 vs 40 mg/Kg LPS (KO, 9-10 weeks)	**0.0079**
10 vs 40 mg/Kg LPS (CT, 5-6 weeks)	0.1490
10 vs 40 mg/Kg LPS (KO, 5-6 weeks)	**0.0450**
9-10 vs 5-6 weeks (KO, 40 mg/Kg)	0.1960

Figure 4. Survival of LPS-treated mice. Control and KO mice aged 9-10 weeks (A) or 5-6 weeks (B) were treated with intraperitoneal administration of LPS, and survival was monitored over 4 days. n indicates the number of animals analyzed in each group. (C) Kaplan-Meier analysis and log rank test were performed to compare survival of mice groups, using the lifetest procedure of SAS version 9.4 (SAS Institute, Cary NC). *P*-values in bold indicate that the survival curves of the indicated group are significantly different.

Figure 5

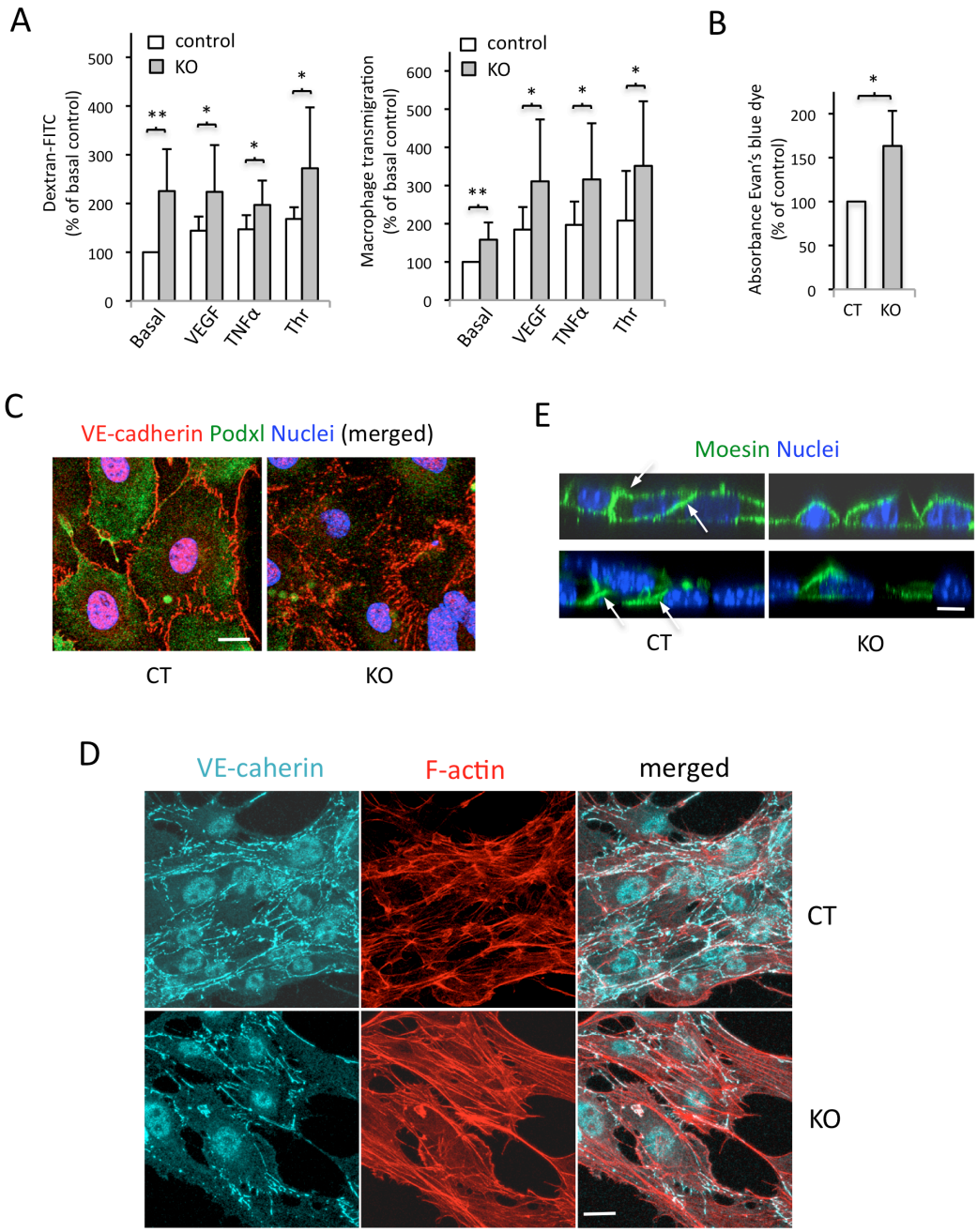

Figure 5. Altered permeability and adherens junctions in Podxl-deficient ECs. (A) Confluent monolayers of MLECs from two control and two KO mice grown in transwells coated with collagen were starved and estimulated for 4 hours with 250 ng/mL VEGF, 100 ng/mL TNFα, or 5 UI/mL thrombin, and permeability to FITC-dextran was measured as described under Methods. In macrophage transmigration assays, MLECs were grown to confluence on gelatin-coated transwells and, then, PU5-1.8 macrophage cells were seeded on top of the transwell and VEGF (250 ng/mL), TNFα (100 ng/mL), or thrombin (5 UI/mL) was added to medium in the lower chamber.

Transmigrated cells were counted as described under Methods. The Anderson-Darling test was used to verify normal distribution of data. Data are expressed as percentage of the value obtained in non-stimulated cells from control mice and represent the mean±SD of four independent experiments. By two tailed, unpaired, t-test: * P<0.05; ** P<0.005. (B) Pulmonary vascular permeability was assessed in five 3-month old control or KO mice as described in Methods. By two tailed, unpaired, t-test: * P<0.02. (C-D-E) Immunofluorescence analysis of Podxl-deficient MLECs. Confluent MLEC cultures from three control and three KO mice were fixed, permeabilized, stained and analyzed in a confocal microscope as described in Methods. (C) Cells were stimulated with 1 IU/mL thrombin for 1 hour before staining with anti-Podxl (green) and anti-VE-cadherin (red). Nuclei were stained with Hoechst (blue). (D) Cells were stimulated with 1 IU/mL thrombin for 1 hour before staining with anti-VE-cadherin (cyan) and phalloidin (red) for F-actin filaments. Nuclei were stained with Hoechst (blue). Scale bars, 10 μm. (E) Confocal xz sections showing enrichment of moesin at the cell-cell contacts in control (arrows) but not in Podxl-deficient cells. Nuclei were stained with DAPI (blue). Representative images of four independent assays.

Figure 6

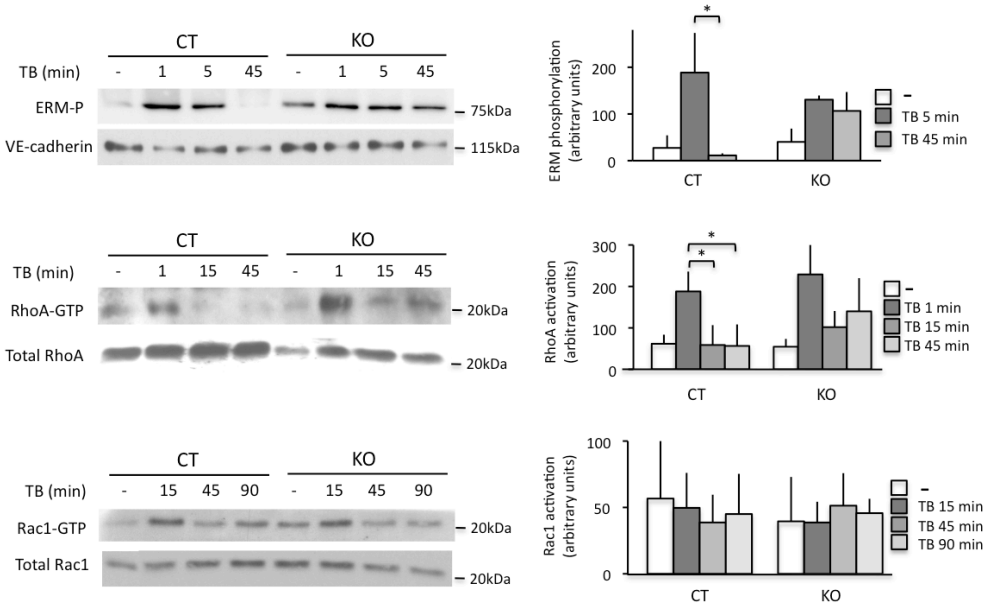

Figure 6. Effect of Podxl-depletion on thrombin-induced ERM phosphorylation and activation of RhoA and Rac1 GTPases. Confluent MLEC cultures from control and KO mice were serum-starved for 2 hours and, then, stimulated with 1 UI/ml thrombin for the indicated times. Western blot

detection of phosphorylated ERM (ERM-P) and active RhoA (RhoA-GTP) and Rac1 (Rac1-GTP) were assessed as described in Methods. Representative experiments are shown and bar graphs represent the mean±SD of four independent experiments. By t-test * $p \leq 0.05$.